

The operation cutoff frequency of high electron mobility transistor measured by terahertz method

Y. M. Zhu and S. L. Zhuang

Citation: [Applied Physics Letters](#) **105**, 011105 (2014); doi: 10.1063/1.4887238

View online: <http://dx.doi.org/10.1063/1.4887238>

View Table of Contents: <http://scitation.aip.org/content/aip/journal/apl/105/1?ver=pdfcov>

Published by the [AIP Publishing](#)

Articles you may be interested in

[Depth-resolved ultra-violet spectroscopic photo current-voltage measurements for the analysis of AlGaIn/GaN high electron mobility transistor epilayer deposited on Si](#)

Appl. Phys. Lett. **105**, 172105 (2014); 10.1063/1.4900869

[Ultrasensitive radio-frequency pseudomorphic high-electron-mobility-transistor readout for quantum devices](#)

Appl. Phys. Lett. **85**, 2956 (2004); 10.1063/1.1790598

[Surface photovoltage spectroscopy of epitaxial structures for high electron mobility transistors](#)

Appl. Phys. Lett. **83**, 2465 (2003); 10.1063/1.1613794

[Indium content measurements in metamorphic high electron mobility transistor structures by combination of x-ray reciprocal space mapping and transmission electron microscopy](#)

J. Appl. Phys. **93**, 4219 (2003); 10.1063/1.1544074

[Universal behavior in irradiated high-electron-mobility transistors](#)

Appl. Phys. Lett. **80**, 2791 (2002); 10.1063/1.1470243

An advertisement for KeySight B2980A Series Picoammeters/Electrometers. The text reads: 'Confidently measure down to 0.01 fA and up to 10 PΩ'. Below this, it says 'KeySight B2980A Series Picoammeters/Electrometers' and 'View video demo >'. To the right is an image of the device and the KeySight Technologies logo.

The operation cutoff frequency of high electron mobility transistor measured by terahertz method

Y. M. Zhu^{a)} and S. L. Zhuang

Engineering Research Center of Optical Instrument and System, Ministry of Education and Shanghai Key Lab of Modern Optical System, University of Shanghai for Science and Technology, No. 516 JunGong Road, Shanghai 200093, China

(Received 16 May 2014; accepted 24 June 2014; published online 7 July 2014)

Commonly, the cutoff frequency of high electron mobility transistor (HEMT) can be measured by vector network analyzer (VNA), which can only measure the sample exactly in low frequency region. In this paper, we propose a method to evaluate the cutoff frequency of HEMT by terahertz (THz) technique. One example shows the cutoff frequency of our HEMT is measured at ~ 95.30 GHz, which is reasonable agreement with that estimated by VNA. It is proved THz technology a potential candidate for the substitution of VNA for the measurement of high-speed devices even up to several THz. © 2014 AIP Publishing LLC.

[<http://dx.doi.org/10.1063/1.4887238>]

With the characteristics of low noise, high power, high efficiency, high frequency, etc.,^{1,2} high electron mobility transistor (HEMT) is one of the most promising applied devices in high frequency millimeter wave and microwave systems. As the operation frequency of HEMTs starts to enter terahertz (THz) region, how to evaluate the cutoff frequency of HEMTs becomes more and more important.

Up to now, the cutoff frequency of semiconductor devices is mainly evaluated by conventional all-electronic, swept-frequency system, which can only detect up to ~ 100 GHz. As assuming the system is linear, we can obtain the cutoff frequency by extrapolation from low frequencies data, which leads to inaccuracy in the cutoff frequency. Furthermore, the vector network analyzer (VNA) that can work in sub-THz region is extremely expensive. To overcome such frequency limitation, a method so called optoelectronic techniques has been employed, which can propose and measure signals up to 700 GHz.^{3,4} However, by using this method, additional fixture and transmission line is needed, which restricts the sample geometry. Furthermore, these fixture and transmission line can also attenuate and distort the measured signal, which causes inaccuracy in measurement and makes signal analysis difficult. So it is very urgent to find a method to cover the bandwidth of high speed devices.

In 2007, Kondo and Hirakawa in Tokyo University got the cutoff of HEMT by combining femtosecond (fs) pulse laser with THz time domain spectroscopy (THz-TDS).⁵ However, their results have some controversies on their THz waveforms radiated from HEMT. In their results, the THz waveforms have a part of negative amplitude values which mean after the deceleration of carriers between the drain and source (due to the instantaneous decrease of drain source current from the shutdown of HEMT caused by the photoexcited carriers between the gate and source electrodes), the carriers are accelerated again, which is un-physics. Here, we think the reasons are following: first, the emitted THz waves

they measured were the waves passing through the HEMT. Although the substrate of HEMT is semi-insulating InP and the buffer layer is undoped InAlAs, after fs laser irradiating between the gate and source, there are a lot of photoexcited electrons and holes. The THz wave emitted from InGaAs/InAlAs layer can be strongly modulated in InAlAs buffer layer and semi-insulating InP substrate, where includes plenty of photoexcited carriers. Second, the THz wave excited from HEMT is like a dipole radiation, the high frequencies part should mainly focus on inner, while the low frequencies part is partly located on the outer which is dispersion very fast. We believe that the distortion of real signal also comes from a part of loss of low frequencies from the process of the signal transmission, from HEMT via parabolics to THz detector.

In this paper, we take the advantage of the ultrafast optics and propose a THz technique based method to investigate the cutoff frequency of HEMT. In this work, we detect the reflected signal from HEMT, which can avoid the modulation by InP substrate and take careful of the distance between HEMT, parabolic mirrors, and THz detector to try our best to avoid the loss of low frequencies part as much as possible. As a result, our experimental data can be logically explained by physics and are well consistent with the design value and experimental result measured by VNA, which means THz method can characterize the cutoff frequency of high speed devices, i.e., HEMT, beyond the frequency range covered by conventional swept-frequency measurements.

The photon generated carriers are induced by irradiating fs laser pulses on the gap between the gate and source electrodes of a biased HEMT sample (Fig. 1(a)), which can make the area photoconductive and short the gate source voltage that causes the step-function like switch off HEMT. Consequently, this induces an ultrafast modulation of the drain source current, I_{DS} , as shown in Fig. 2(a) without considering the electrons scattering in side of sample, which results in the radiation of THz electromagnetic waves whose electric field $E_{THz}(t)$ is proportional to $\partial I_{DS}/\partial t$ as shown in Fig. 2(b). By measuring the waveform of THz radiation from the HEMT, which contains the information on the transition

^{a)}Author to whom correspondence should be addressed. Electronic mail: ymzhu@usst.edu.cn.

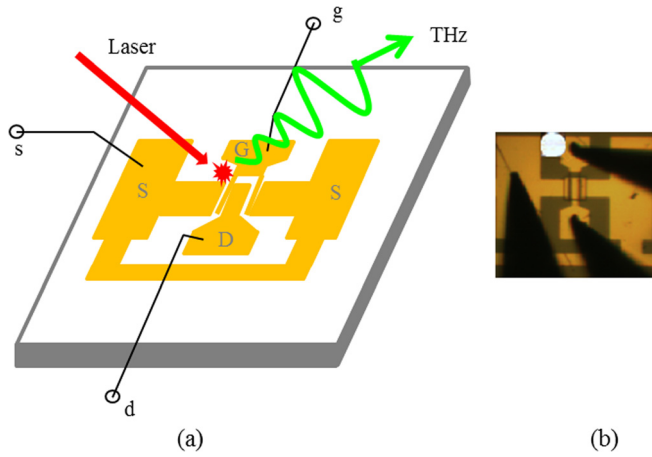


FIG. 1. (a) Schematic diagram of the position of three probes in HEMT device; (b) The actual experimental HEMT, laser spot, and three probes.

time of carriers between the drain and source electrodes modulated by the gate electric field, the cutoff frequency of HEMT can be obtained.^{5,6}

The sample we use in this work is depletion-type $\text{In}_{0.53}\text{Ga}_{0.47}\text{As}/\text{In}_{0.52}\text{Al}_{0.48}\text{As}$ HEMT grown on semi-insulating InP substrate. The gate length L_g of HEMT sample is $0.4 \mu\text{m}$, the density of 2D electron gas is $3.32 \times 10^{12} \text{cm}^{-2}$, the transconductance is 600mS/mm , the maximum current density is 500mA/mm , and the electron mobility is $9290 \text{cm}^2/(\text{Vs})$, which is provided by Institute of Microelectronics of Chinese Academy of Science.⁷ In such kind of device, the dynamics of carriers should not be a diffusive motion but a ballistic acceleration motion.⁸ Therefore, the cutoff frequency of HEMT is determined by the transition time of electrons between the source and drain, which is mainly determined by the gate length (L_g) and electron mobility of HEMT.⁹

Figure 3 shows the experimental setup. The fs laser we use is Ti: sapphire fs laser whose central wavelength is 800nm , the pulse duration is 80fs , and the repetition rate is 76MHz . As shown in the figure, the laser is split to a pump beam and a probe beam by a beam splitter. The pump beam, which is just 8mW , is focused on the gap between the gate and source electrodes of HEMT sample. Since the photon energy of laser pulse $\sim 1.55 \text{eV}$ is larger than the band gap of $\text{In}_{0.7}\text{Ga}_{0.3}\text{As}$, the pump pulses make the gap between the gate and source pads photoconductive and, consequently, the gate-source voltage is suddenly shunted. Then, the THz waves emitted from the sample are collected by off-axis parabolic mirrors, and together with the probe beam, are focused on zinc telluride (ZnTe)

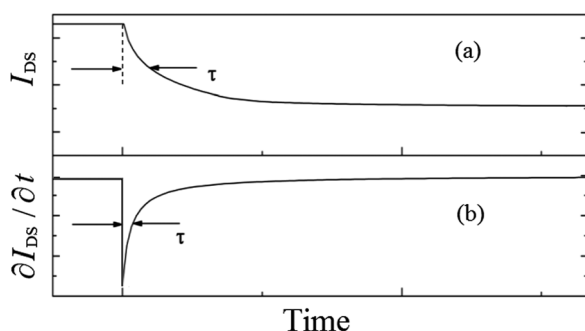


FIG. 2. Time dependence of the source drain current I_{DS} and $\partial I_{DS}/\partial t$.

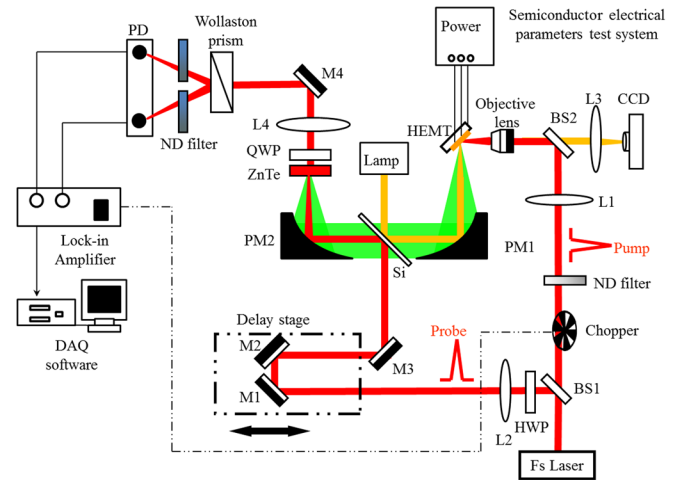


FIG. 3. THz-TDS system with reflecting mirrors (M1–M7), lenses (L1–L4), off-axis parabolic mirrors (PM1–PM4), beam splitter, high resistant silicon wafer (Si), half-wave plate (HWP), quarter-wave plate (QWP), and Wollaston prism.

electro-optic (EO) crystal, and the waveform of the THz wave is recorded by the free space EO sampling technique.^{10,11} In this experiment, the ZnTe for the THz detection is a $700 \mu\text{m}$ -thick and $\langle 110 \rangle$ -oriented crystal, whose cutoff frequency can reach $\sim 2 \text{THz}$.¹² Objective lens, Charge Coupled Device (CCD) camera, and white light source are used for observation of the laser spot and the position of three probes, which were added on the gate, source, and drain electrodes of our HEMT devices.

By adjusting the position of HEMT, we make the laser spot focuses on the gap between the gate and source electrodes. Figure 1(a) is the schematic diagram shows the position of laser spot and three probes on HEMT. We supply gate source voltage V_{GS} by using probe g and probe s, which lead out from the gate source electrode G and source electrode S, respectively, and supply drain-source voltage V_{DS} by using probe d and probe s, which lead out from gate source electrode D and source electrode S, respectively. Furthermore, Fig. 1(b) is photograph from the real experiment, and we can see the structure of HEMT, the laser spot on our HEMT (bright spot), and three probes (black shadow).

The I - V characteristics of HEMT before and after laser irradiation under different bias gate source voltages (V_{GS}) are shown in Fig. 4. From the figure, we can see that the drain source current, I_{DS} , changes when HEMT works under different bias gate source voltages V_{GS} and drain sources V_{DS} . The solid line represents the I_{DS} without fs laser irradiation, while the dotted line represents the I_{DS} under laser irradiation. In principle, with laser irradiation, the HEMT should be closed, which causes the I_{DS} to be almost zero for direct current (DC) measurement. However, as shown in figure, the difference between the I_{DS} with and without laser irradiation is relative small. This is because the duration of fs laser pulses is very short,¹³ and in most of time, the HEMT sample is under a no-irradiated state, and the average reduction of the source drain current I_{DS} is not very obvious. Furthermore, from the curves we also can see that the difference of the I_{DS} with/without laser irradiation can only happen when the HEMT works in the relatively high drain

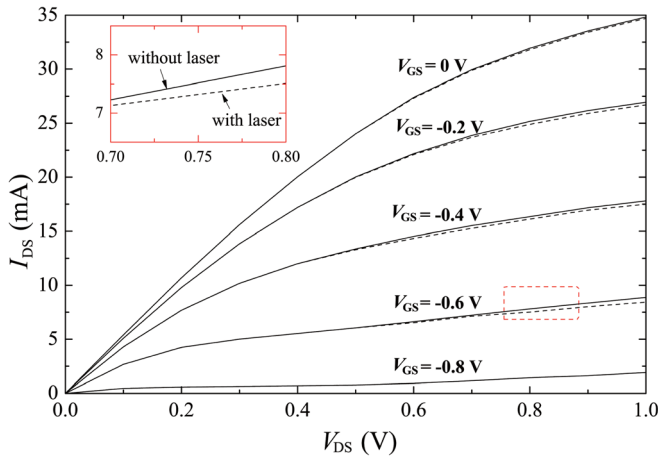


FIG. 4. I - V characteristics of HEMT before and after laser irradiation, and the inset is the detail of the dotted rectangular area.

source voltage area (saturation region), such as $V_{DS} > 0.6$ V, in which the HEMT device can work very well.

The experimental results of the THz waveforms emitted from our HEMT sample are shown in Fig. 5. The curve (a) (the top one) is the HEMT sample not working in saturation region (instauration state: $V_{DS} = 0.2$ V, $V_{GS} = -0.6$ V), and the curve (b) (the bottom one) is the sample working in saturation area (saturation state: $V_{DS} = 0.8$ V, $V_{GS} = -0.6$ V). The figure tells us that only HEMT in saturation state can radiate THz after laser irradiation. This fact clearly shows that the observed THz radiation does not originate from carrier drift in parasitic depletion regions in the samples but is due to the change in I_{DS} by optical modulation of the gate electric field. Our measured THz trace is consistent with our expected result as shown in Fig. 2(b) well and is different from the result obtained by Kondo and Hirakawa, which exists a THz peak and an un-physical THz dip that cannot be explained.⁵ Then, it is reasonable to believe that the information on transient time, τ , in I_{DS} is contained in the THz waveforms.¹³ We estimated τ of our HEMT sample in I_{DS} from the half-width of the measured THz waveforms shown in Fig. 5, which is 1.67 ps, and the cutoff frequency can be

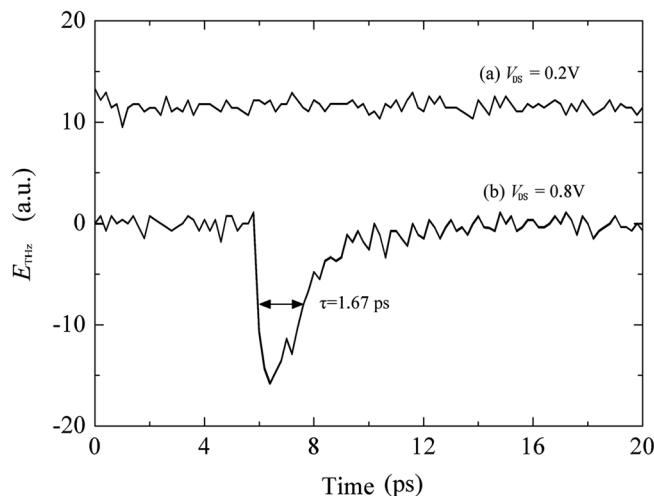


FIG. 5. The radiation of THz wave from our HEMT sample, (a) the HEMT sample under instauration state: ($V_{DS} = 0.2$ V, $V_{GS} = -0.6$ V) and (b) the HEMT sample under saturation state: ($V_{DS} = 0.8$ V, $V_{GS} = -0.6$ V).

TABLE I. The cutoff frequency of our HEMT (design frequency, THz-TDS measurement, and network analyzer measurement).

Design Cutoff frequency f_T (GHz)	THz-TDS Cutoff frequency f_T (GHz)	Network analyzer Cutoff frequency f_T (GHz)
94	95.30	87

deduced from this carrier dynamics time, which should be $f_T = 1/(2\pi \times 1.67 \times 10^{-12}) = 95.30$ GHz.^{5,6}

We also use the VNA to verify the cutoff frequency of our HEMT sample. Table I shows the design frequency of our HEMT and the experimental results from THz-TDS method as well as VNA measurement. The slight difference between two experimental results may be come from the inaccuracy in extrapolation method by VNA, whose limitation frequency is just 67 GHz. The similar measurement results indicate that the THz method could be a candidate to take place of VNA to evaluate cutoff frequencies of ultrafast transistors or devices.

In conclusion, from the emitted THz waveform due to ultrafast change in drain current induced by optical gate-field modulation, we can obtain the cutoff frequency of HEMT directly. The THz method agrees well with the VNA measurement result and the design frequency. Furthermore, our THz method does not need any extrapolation, which leads to inaccuracy in the cutoff frequency, and additional fixture and transmission line, such as optoelectronic techniques. Therefore, THz-TDS system is a potential candidate for the substitution of VNA in future for the measurement and calibration of high-speed devices even up to several THz.

This work was partly supported by National Program on Key Basic Research Project of China (973 Program, 2014CB339806), National Natural Science Foundation of China (11174207 and 61138001), Major National Development Project of Scientific Instrument and Equipment (2011YQ150021 and 2012YQ14000504), Program of Shanghai Subject Chief Scientist (14XD1403000), and Basic Research Key Project (12JC1407100).

¹N. Hara, K. Makiyama, T. Takahashi, K. Sawada, T. Arai, T. Ohki, M. Nihei, T. Suzuki, Y. Nakasha, and M. Nishi, *IEEE Trans. Semicond. Manuf.* **16**(3), 370 (2003).

²T. Otsuji, Y. Imai, E. Sano, S. Kimura, S. Yamaguchi, M. Yoneyama, T. Enoki, and Y. Umeda, *IEEE J. Solid-State Circuits* **32**, 1363 (1997).

³M. Y. Frankel, *Opt. Quantum Electron.* **28**, 783 (1996).

⁴T. Nagatsuma, M. Shinagawa, N. Sahri, A. Sasaki, Y. Royter, and A. Hirata, *IEEE Trans. Microwave Theory Tech.* **49**, 1831 (2001).

⁵T. Kondo and K. Hirakawa, *Appl. Phys. Lett.* **91**, 191120 (2007).

⁶S. M. Sze, *Physics of Semiconductor Devices* (Wiley-Interscience, New York, 1981).

⁷J. X. Bian, Y. M. Zhu, X. X. Jia, L. Chen, Y. Peng, Y. C. Yang, and S. L. Zhuang, *Front. Optoelectron.* **4**, 444 (2011).

⁸J. G. Ruch, *IEEE Trans. Electron Devices* **19**(5), 652 (1972).

⁹T. Suemitsu, T. Enoki, and H. Yokoyama, *Jpn. J. Appl. Phys., Part 1* **37**, 1365 (1998).

¹⁰Q. Wu and X. C. Zhang, *Appl. Phys. Lett.* **71**, 1285 (1997).

¹¹Y. M. Zhu, T. Unuma, K. Shibata, and K. Hirakawa, *Appl. Phys. Lett.* **93**, 042116 (2008).

¹²Q. Wu and X. C. Zhang, *Appl. Phys. Lett.* **70**, 1784 (1997).

¹³M. Y. Frankel, J. F. Whitaker, and G. A. Mourou, *IEEE J. Quantum Electron.* **28**, 2313 (1992).